УДК 629.4

I.Y. SHEVTSOV, V.L. MARKINE, C. ESVELD
Delft University of Technology (The Netherlands)

DESIGN OF RAILWAY WHEEL PROFILE USING OPTIMIZATION TECHNIQUE

Створено процедуру дизайну профілю колеса, яка заснована на геометричних характеристиках контакту колеса і рейки. Використовуючи чисельну техніку оптимізації, був одержаний профіль колеса з заздалегідь визначеними геометричними властивостями контакту. Показано, що одержаний профіль колеса може зменшувати знос колеса і рейки без погіршення динамічних показників. Остання властивість була проаналізована з використанням обчислювального пакета ADAMS/Rail.

Создана процедура дизайна профиля колеса, основанная на геометрических характеристиках контакта колеса и рельса. Используя численную технику оптимизации, был получен профиль колеса с заранее определенными геометрическими свойствами контакта. Показано, что полученный профиль колеса может уменьшать износ колеса и рельса без ухудшения динамических показателей. Последнее свойство было проанализировано с использованием вычислительного пакета ADAMS/Rail.

A wheel tread design procedure has been developed. The procedure is based on the geometrical characteristics of hie wheel and rail contact. Using the numerical optimization technique we have got a wheel tread with the contact geometrical characteristics that were determined in advance. It has been show that the obtained wheel tread can reduce wheel and rail wear not worsening the dynamic characteristics. The latter, property has been analyzed with the hel the computation package ADAMS/Rail.

Introduction

During the last decades substantial progress has been made in design of railway vehicles and running gears. Tilting trains, high speed trains, active steering wheelsets and many other sophisticated solutions have been implemented in recent years on the railways. But despite this progress, the mechanics of railway wheelset remains the same and an inappropriate combination of wheel and rail profiles can easily diminish all this technological advances. Besides, many old fashioned vehicles are still in too good condition to be replaced. They have a special need for appropriate combinations of wheel/rail profiles since such vehicles do not have high-tech devices which improving performance.

Wheel profile design is an old problem and different approaches have been developed to obtain satisfactory combination of wheel and rail. It is possible to find an optimal combination of wheel and rail profile when dealing with closed railway system, i.e. when only one type of rolling stock is running on track system and no influence of other types of railway vehicles is present. Examples of such systems are heavy haul and tram lines. In the present paper a closed system is considered, namely a new wheel profile is designed for vehicles running on tram line in The Hague.

By studying geometrical characteristics of a contact between wheel and rail it is possible to judge about dynamic behaviour of the wheelset and ultimately about dynamic parameters of the vehicle since a wheelset represents a source of disturbances from a track to a vehicle. The wheel and rail geometry plays a dominant role in lateral vehicle dynamics. When a wheelset travels along a track the centre of the axle makes sinusoidal movements. The rolling radii, the contact angles and the wheelset roll angle vary as the wheelset moves laterally relative to the rails. The nature of the functional dependence between these geometrically constrained variables and the wheelset lateral position is defined by the cross-sectional shape of the wheel and rail. One important characteristic of the wheel-rail contact is the rolling radius of a wheel at the contact point [1], which in fact is different for the right and left wheel (r_1 and r_2, respectively, see Fig. 1). When a wheelset is in a central position, the rolling radii of both wheels are the same, i.e. $r_1 = r_2 = r$. An instantaneous difference between rolling radii of the right and left wheels, i.e. $\Delta r(y) \equiv r_1(y) - r_2(y)$ is defined as a function of the lateral displacement y of the wheelset with respect to the central position. An example of a rolling radii difference (RRD) for conical and worn profiles (also known as a '$y - \Delta r$' curve) is shown in Figure 2. Generally, it is a non-linear function of the lateral displacement y of a wheelset. Due to the wear of

wheels the wheel profile is changing and consequently the function $\Delta r(y)$ is changing as well as shown in Figure 2. The difference between the rolling radii of the left and right wheels of the wheelset is present in the equations of motion of the wheelset. The RRD is one of the main characteristics that describes the contact between wheelset and railway track, which in turn defines the dynamic behaviour of a wheelset [1], [2].

Determination of geometric contact characteristics for given wheel and rail profiles, wheel and rail gauge, and railhead cant angles is a well-known problem already solved for many years. These nonlinear characteristics have been investigated by Wickens [3], Cooperrider [4] and De Pater [5]. A linear conical wheel profile widely used earlier has discontinuous linear characteristics of rolling radii difference, see Figure 2, that results in shocks during a contact between wheel flange and rail during movement of wheelset. On the other hand worn wheel better match the rail, and therefore usually has smoother RRD function. However, high conicity of a worn wheel reduces the critical speed of a wheelset and results in strong oscillations of the vehicle. Naturally, there is a desire to find a compromise between these two extreme situations. A traditional way to achieve such a compromise is by using a trial and error approach while modifying a wheel profile in order to obtain satisfactory contact characteristics for a given rail. Usually wheel should satisfy curve passing, hunting, and allowable contact stresses conditions. However, this is quite time consuming and ineffective way.

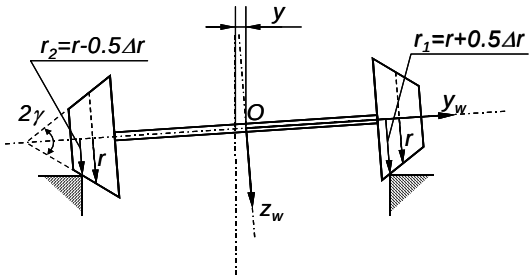

Fig. 1. Rolling radii (r_1 and r_2) corresponding to positive wheelset displacement y . Wheels are shown conical with conicity ε . Wheelset coordinate $Oy_w z_w$ system also shown

A more efficient approach is to use numerical solution of an inverse problem, i.e. design of a wheel profile based on a given rolling radii difference Δr and rail profile. If a function of rolling radii difference $\Delta r(y)$ for the wheelset and the rail profile is known, one can try to find the corresponding wheel profile. However, there is no direct way to solve this problem. Here, the problem of determination of the wheel profile for a given RRD function and rail profile has been formulated as an optimization problem. This problem, solution method and numerical results are described in the sequent sections.

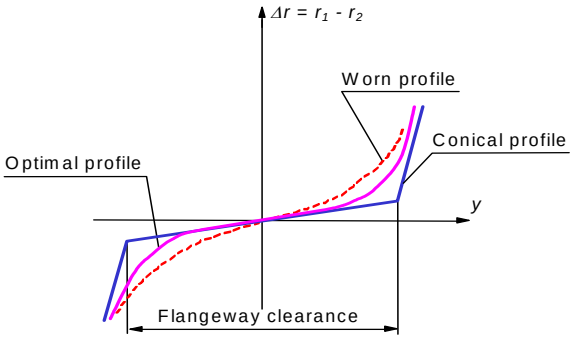

Fig. 2. Rolling radii difference vs. lateral displacement of wheelset (' $y - \Delta r$ ' curve)

1. Design procedure

The procedure of wheel profile design consists of several steps. It starts from the definition of the target RRD function. For this purpose, wheel and rail profile measurements are used to collect data on new and worn profiles. The next step is to process these data and convert them to a form, which will be used during the design of a wheel profile. Thus, the RRD curves for different wheel and rail combinations have been analysed and the target RRD function has been obtained. After this stage the optimization problem has to be formulated and solved which results in a new wheel profile. The obtained profile should be checked regarding dynamic performance and satisfaction of the wear and safety requirements. Here, vehicle dynamic simulations have been performed using ADAMS/Rail software. If this test fails the optimization procedure has to be repeated with new target RRD and the dynamic simulation has to be performed again. However, for a successful simulation the corresponding wheel profile is taken as the optimum one.

A target rolling radii difference function can be obtained in several ways.

- It can be a modification of a rolling radii difference function for an existing wheel profile.
- One can use the average RRD curve for worn wheels.
- It can be built based on designer's experience.

All these concepts will be discussed in details in the following sections.

2. Formulation of optimization problem

To make use of numerical optimization techniques an optimization problem should be stated in a general form that reads:
Minimize

$$F_0(\boldsymbol{x}) \to \min, \quad \boldsymbol{x} \in R^N \qquad (1)$$

subject to

$$F_j(\boldsymbol{x}) \le 1, \quad j = 1,...,M \qquad (2)$$

and

$$A_i \le x_i \le B_i, \quad i = 1,...,N \qquad (3)$$

where F_0 is the objective function; F_j, $j = 1,...,M$ are the constrains; $\boldsymbol{x} = [x_1,...,x_N]^T$ is the vector of design variables; A_i and B_i are the side limits, which define lower and upper bounds of the i-th design variable.

The components of the vector $\boldsymbol{x}$ can represent various parameters in a mechanical design problem, such as geometry, material, stiffness and damping properties. These can be varied to improve the design performance. Depending on the problem under consideration, the objective and constraint functions, see equations (1) and (2), can describe various structural and dynamic response quantities such as weight, reaction forces, stresses, natural frequencies, displacements, velocities, accelerations, etc. Also cost, maintenance and safety requirements can be used in the formulation of the optimization problem. The objective function provides a basis for improvement of the design whereas the constraints impose necessary limitations on the properties or behaviour of the structure.

Formulated in the form (1)-(3), the optimization problem can be solved using a conventional method of Nonlinear Mathematical Programming (NMP).

2.1. Design variables

To describe the wheel profile several points on the flange, the flange root and the wheel tread have been chosen. Connected by a piecewise cubic Hermite interpolating polynomial, these points define the shape of the wheel profile, as shown in Figure 3. The position of these points can be varied in order to obtain an optimum profile. To reduce the optimization time the points on the flange top and on the conical part of the profile, which do not participate in the contact, have been fixed, see Figure 3. The lateral positions of the other points (moving points) have been fixed while their vertical positions have been varied. The vertical coordinates of the moving points have been chosen as the design variables. During the initial computations the number of the moving points on the wheel profile and their positions along the horizontal axis has been determined. In general case vector of design variables for wheel profile can be written as,

$$\boldsymbol{x} = [z_1,...,z_N], \qquad (4)$$

where z_i are the vertical coordinates of the moving points. They are located along the wheel flange, the flange root and the tread as shown in Fig. 3.

2.2. Objective function

The requirement reflecting the minimum discrepancy between the target function of the rolling radii difference $\Delta r(y)$ and the RRD function for the design wheel profile can be written as:

$$F_0(\boldsymbol{x}) \equiv \frac{\sum_{i=1}^{K}\left(\Delta r^{tar}(y_i) - \Delta r^{calc}(\boldsymbol{x}, y_i)\right)^2}{\sum_{i=1}^{K}\left(\Delta r^{tar}(y_i)\right)^2} \to \min, \qquad (5)$$

where Δr^{tar} is the target rolling radii difference function; Δr^{calc} is the calculated rolling radii difference function for the design profile; y_i is the coordinate of the point of the lateral displacement of the wheelset; K is the number of such points.
The function (5) has been taken as the objective function of the optimization problem (1) - (3). The other requirements to optimum wheel profile have been considered as constrains (2). They are discussed below.

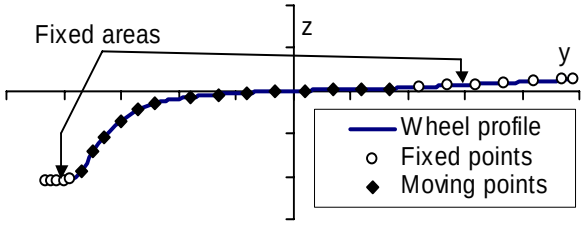

Fig. 3. Wheel profile, moving and fixed points

2.3. Requirements

Equivalent (or effective) conicity γ_e [1], [2] is considered as the parameter defining stability of the wheelset. For different types of railway vehicles, wheels with different equivalent conicity should be used to achieve required critical speed. High conicity can result in dynamic instability or "hunting" of the vehicle, which severely

deteriorates its ride characteristics and can seriously damage the track. The equivalent conicity limit value $\gamma_e^{\max}$ for a wheel was set to avoid too high conicity of a new wheel that reads:

$$F_1 \equiv \left(\gamma_e^{\max} - \gamma_e\right) \Big/ \gamma_e^{\max} \geq 0 . \qquad (6)$$

Two safety requirements have been considered. The first one is the requirement for wheel flange thickness, which is checked after the optimization. The second one is the requirement to avoid derailment of the vehicle which is achieved by the restriction on the minimal flange angle. This requirement has been checked for the optimized profile as well.

Constrains on angles between the adjacent parts of profile were introduced to avoid zigzags of wheel profile and thus to exclude unrealistic wheel designs during optimization. Moving points have been numbered from 1 to N, starting from the low left side to the upper right of profile, see Figure 3. Constrains for point number i is written as

$$F_j \equiv 1 - \gamma_{i+1}/\gamma_i \geq 0 , \; j = 2,...,k, \qquad (7)$$

for the concave part of the profile. Accordingly for the convex part of the profile these requirements read:

$$F_j \equiv 1 - \gamma_i/\gamma_{i+1} \geq 0 , \; j = k+1,...,N+1. \quad (8)$$

The γ_i is the angle between the y_w-axis of the wheelset (see Fig. 1) and the straight line connecting points i and $i+1$ of the wheel profile. Some moving points located on the flange can be absent in (7)-(8), since their positions had been already constrained by the side limits (3).

3. Optimization method

The problem (4) – (8) has been solved using the MARS method (Multipoint Approximation based on Response Surface fitting) [6], [7]. The method has been specifically developed for problems where multiple response analyses and (time consuming) simulations are involved.

The MARS method is based on the approximation concepts [7], [8], [9] according to which the original minimization problem is replaced with a succession of simpler ones formulated for approximations of the original objective and constraint functions.

According to the MARS method, each approximation $\widetilde{F}$ is defined as a function of the design variables **x** and tuning parameters **a**. To determine the components of the vector **a**, the following weighted least-squares minimization problem is to be solved:

Find vector **a** that minimizes

$$G(\boldsymbol{a}) = \sum_{p=1}^{P} \{w_p [F(\boldsymbol{x}_p) - \widetilde{F}(\boldsymbol{x}_p, \boldsymbol{a})]^2\} . \quad (9)$$

Here $F(\boldsymbol{x}_p)$ is the value of the original function evaluated at the point of the design parameter space $\boldsymbol{x}_p$, and P is the total number of such points; w_p is a weight factor that characterizes the relative contribution of the information about the original function at the point $\boldsymbol{x}_p$. The main issues of the MARS method such as type of approximation functions, planning of numerical experiments and move limit strategy are out of scope of the paper. More information about the weight coefficient assignment, the move limits strategy and the most recent developments in the MARS method can be found in [6], [7], [10].

4. Dynamic analysis

When the optimization problem has been solved, the dynamic performance of the vehicle, with the obtained wheel profile, has to be checked. The tramcar studied here was modelled using the ADAMS/Rail computational package. An internal ADAMS/Rail procedure has been used for calculation of the wear index. The wear index W, taken from the English Normatives (British Rail), is calculated as

$$W = F_1 \cdot \xi + F_2 \cdot \eta \qquad (10)$$

where F_1 is the longitudinal creep force; ξ is the longitudinal creepage; F_2 is the lateral creep force; η is the lateral creepage (also see [11]).

In all presented cases, the tram simulations have been performed on the track consisting of 50 m straight track continuing into 40 m transition curve, then switching into the 50 m right turn curve with R=150 m and 30 m transition curve and ending with 230 m straight track. The vehicle travels with the speed of 10 m/s.

The wear index W in (10) on the left wheel of the first wheelset and the lateral displacement y of the first wheelset have been chosen as the most representative quantities in the dynamic check. Based on the lateral displacements one can judge about the stability of wheelset.

5. Numerical results and discussion

For design of wheel profiles for given rolling radii difference function a procedure has been developed. The design procedure was applied to

design of tram wheel profile. In the present calculations, the rail S49 with inclination 1:40 is used. The wheel profiles HTM2 (used by HTM - The Hague tram company) and S1002 have been chosen as reference profiles. The track has normal 1435 mm gauge, the wheelset inner gauge is 1385 mm.

Here the target function designed basing on the RRD function for non-worn profiles has been considered. The case with target function based on designer experience is described in [12] and the case when the mean RRD curve (calculated for the set of RRD curves for measured wheel/rail profiles) has been used as a target function is described in [13].

For analyzes of geometrical contact properties the contact situation between the wheel and rail for various lateral displacements of wheelset has been considered. The contact situation for HTM2 and S1002 wheels on S49 rail are shown in Figure 4 and Figure 5 correspondingly. The lines between the wheel and the rail profiles connect the corresponding contact points and values of corresponding lateral displacements of the wheelset are shown above the wheel profile. The wheel profile has been lifted over the rail on 10 mm. The rail profile arranged in his real position, the coordinate system on this figure is wheelset coordinate system (see Fig. 1) with origin in the centre of the wheelset when it placed in neutral position. For the unworn tram wheel HTM2 on the rail S49 with inclination 1:40 contact points are spread on the top of rail and on wheel tread up to 3 mm of the wheelset lateral displacement (see Fig. 4). Between 3.5 and 5 mm of lateral displacement wheel has the contact on the flange root. Flange contact appears at 5.5 mm of lateral displacement and located on the top of the flange. For the S1002 wheel contact on the tread part is similar to the contact of the HTM2 wheel, but on the flange the situation is totally different as shown in Figure 5. Comparing Figure 4 with Figure 5 one can see that contact points are located almost on the top of the flange of HTM2 wheel whereas for S1002 wheel the contact points are spread along the flange. But for the S1002 wheel the jump from the tread to the flange still must be reduced.

In Figure 6 the rolling radii difference (RRD) functions for all combinations of the wheel and rail profiles are presented. The RRD function of the HTM2 profile on rail S49 is increasing with increase of the lateral displacement of wheelset until the point +/-5 mm after which the RRD function sharply increases. From 6 mm HTM2 wheel has top flange contact and RRD function is almost constant. S1002 wheel profile has different RRD functions as compared to the HTM2 wheel profile. Transition from the flange root to the flange is smoother for the S1002 profile than for HTM2.

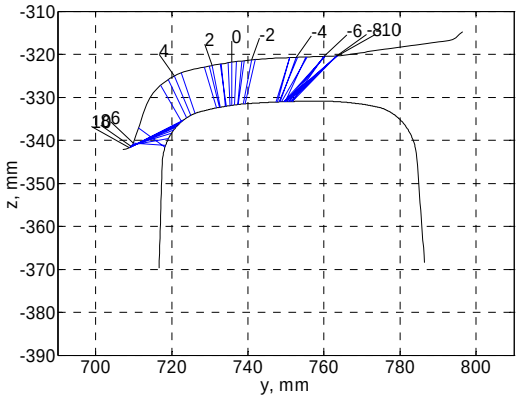

Fig. 4. Position of contact points on HTM2 wheel and S49 rail depending on lateral displacement of wheelset

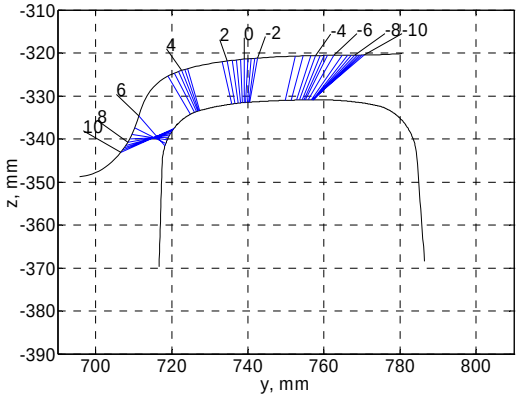

Fig. 5. Position of contact points on S1002 wheel and S49 rail depending on lateral displacement of wheelset

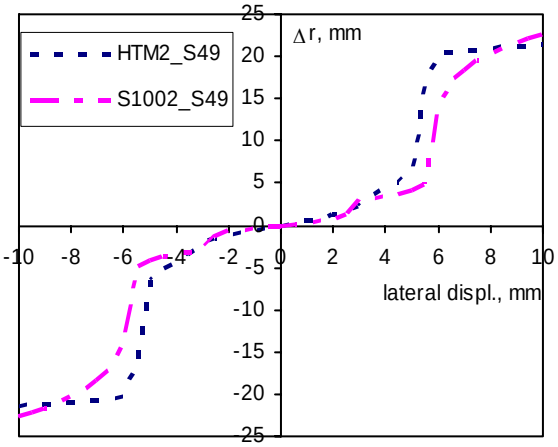

Fig. 6. RRD functions for the HTM2 and S1002 wheel profiles on S49 rail

For the S1002 wheel the RRD function is divided on three regions, as can be seen in Figure 6. The first one is corresponding to the tread

contact (+/-2.5 mm), the second one corresponds to the flange root contact (+/-3-5.5 mm) and the third one is related to the flange contact (after +/-6 mm). The first region is responsible for the motion on the straight track, the second one is responsible for the curves with large radius and the third one is responsible for sharp curves. Such division provides necessary RRD for stability on the straight track and passing curves. On a straight track the RRD should not exceed certain value to have required critical speed, dependent from the type of the vehicle. On a large radius curves wheelset will have steady motion because RRD provides stable region for certain range of lateral displacement (+/-3-5.5 mm).

The S1002 wheel and S49 rail have very good contact properties of contact on the tread part of the wheel. The contact properties of the flange contact are less good for this wheel/rail combination. A big jump of contact point from the tread to the flange has been observed. A decision has been made to use S1002 profile as the starting profile in optimization and improve the flange contact of this profile. The modified RRD of the S1002 wheel and S49 rail has been used as a target function. As it can be seen from Figure 7, from 0 to 5.5 mm of lateral displacement RRD function of the S1002/S49 combination has been left without changes. After 5.5 mm up to 10 mm of lateral displacement of wheelset target RRD function is smooth to achieve smooth flange contact. The end point of the target RRD is placed lower than the end point of S1002/S49 RRD function and almost coincides with the end of the RRD function for HTM2/S49 combination. This is because the flange of S1002 profile is longer than the flange of the tram wheel (see Figure 4 and Figure 5). As a result the RRD for the top flange contact is higher for S1002 profile. In the optimization problem here 21 mm flange height of tram wheels is used. Therefore the RRD values should coincide for top flange contact of wheels with the same flange height, see “Target” and “HTM2_S49” lines at 10 mm of lateral displacement.

The results of the optimization are presented in Figure 7 and Figure 8. Comparing the wheel profiles in Figure 8 one can see that flange angle of the optimized profile (Opt26f) has been reduced and flange root radius has been increased. Also on the field side of the tread, lower conicity has been introduced as compared to HTM2 profile. The optimization has been performed for the range 5.5-8 mm of lateral displacement of the wheelset as described earlier. On Figure 7 lines “Target” and “opt26f_S49” are very close to each other in the range 5.5-8 mm. The relatively large difference between these two lines after 8 mm of lateral displacement is not important because the corresponding top flange contact has not been taken into account in the optimization.

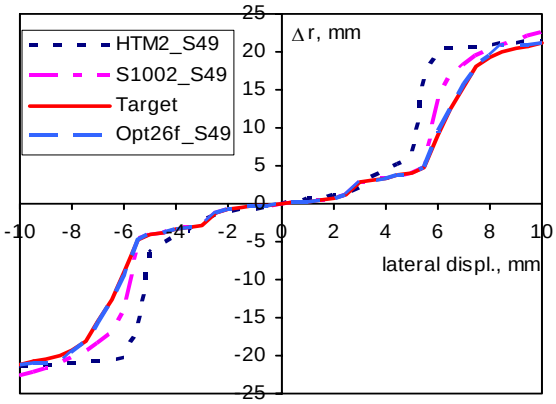

Fig. 7. RRD functions for the HTM2, S1002 and Opt26f wheel profiles on S49 rail and target RRD function

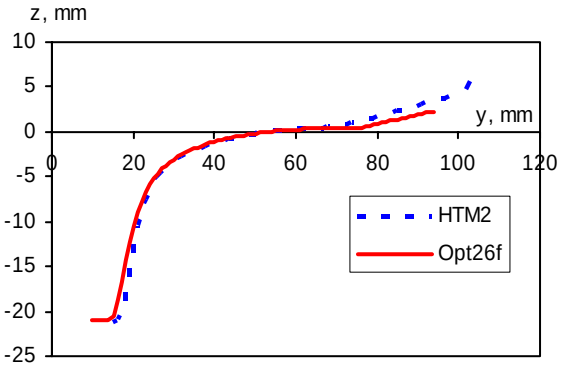

Fig. 8. Initial (HTM2) and optimized (Opt26f) wheel profiles.

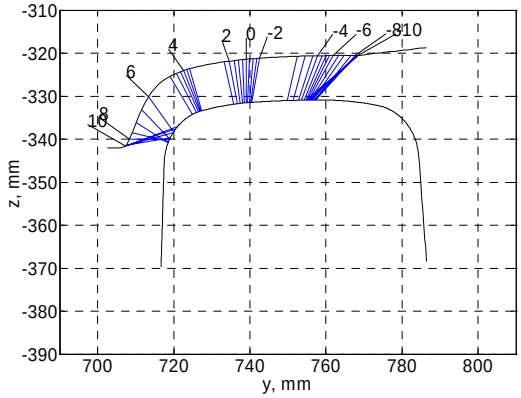

Fig. 9. Position of contact points on Opt26f wheel and S49 rail depending on lateral displacement of wheelset

Let us compare contact situation for Opt26f wheel profile shown on Figure 9 with contact situation for HTM2 wheel profile shown on Figure 4. For Opt26f profile contact points on the flange are evenly spread along the flange in

contrast to the contact situation on the flange of HTM2 profile where contact is moved to the flange top part. Such evenly spread contact will allow bigger variety of RRD. This will provide the possibility to find radial position for the wheelset and accordingly wheel flange wear will decrease.

Dynamic simulations of the tram running on the straight track with the speed of 20 m/s have been performed to check stability of the designed wheel. This speed is the maximum operational speed of a tram and it is below the critical speed. After passing the lateral ramp the oscillations of the wheelset have been damped out fast. Hence tram is stable on unworn wheel profiles. Lower conicity of the Opt26f profile leads to smaller lateral displacement of the wheelset, as compared to the HTM2 profile. As a result the wear index is smaller. Therefore the tram with optimized profile will produce less wear on the straight track.

After stability analysis the tram simulations on a curved track have been performed. The radius of the curve is 150 m, simulations for smaller radius curves cannot be performed due to restrictions of the vehicle model. Results of dynamic simulation of the tram running with the speed of 10 m/s are presented on Figure 10 and Figure 11. The initial position of the first wheelset in the tram model is situated at the distance of 24 m from the beginning of the track. This is done to accommodate complete vehicle on the track. Consequently the first wheelset have to travel only 26 m until the beginning of the first transition curve. This means that with the speed of 10 m/s in 2.6 s first wheelset is passing straight part of the track. The first transition curve is passed by first wheelset in 4 seconds from 2.6 s till 6.6 s. On track with constant radius the first wheelset will run 5 seconds from 6.6 s till 11.6 s. The second transition curve will be passed in 3 seconds from 11.6 s till 14.6 s. Last 10.4 seconds from 14.6 s till 25 s the first wheelset will run on the straight track.

Analyzing Figure 10 one can see that the lateral displacement of the wheelset with HTM2 wheel profile is growing from 0 mm on the straight track to 4.9 mm on the constant radius curve (6.6-11.6 sec). On the second transition curve (11.6-14.6 sec) the lateral displacement increases up to 5.3 mm. The lateral displacement of the wheelset with profile Opt26f on the constant radius curve is equal to 5.7 mm and on the second transition curve is 6.7 mm. In the constant radius curve both profiles have contact on the flange root. The contact point of the Opt26f profile for 5.7 mm of lateral displacement (see Fig. 9) is situated closer to the flange (higher conicity) than the HTM2 profile at 4.9 mm of lateral displacement (see Fig. 4). That is why the wear index is slightly higher for the Opt26f profile in the constant radius curve than for HTM2 profile as shown on Figure 11.

On the second transition curve the situation became opposite. The lateral displacement of the wheelset with HTM2 profile is 5.3 mm, which is smaller than the lateral displacement for Opt26f profile which equal to 6.7 mm. But, because of the absents of the contact on the flange the contact point on HTM2 profile is situated on the top of the flange whereas the contact point of the Opt26f profile is situated in the middle of the flange (also see Fig. 4 and Fig. 9). This means that HTM2 profile will have heavy flange contact which will result in higher wear rate as one can see on Figure 11.

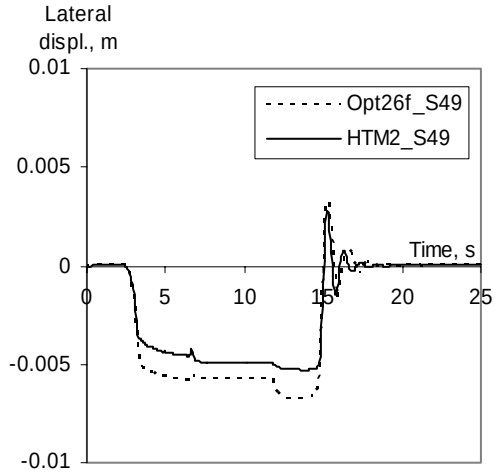

Fig. 10. Lateral displacements of front wheelset vs. time. Opt26f and HTM2 wheels are on S49 rail

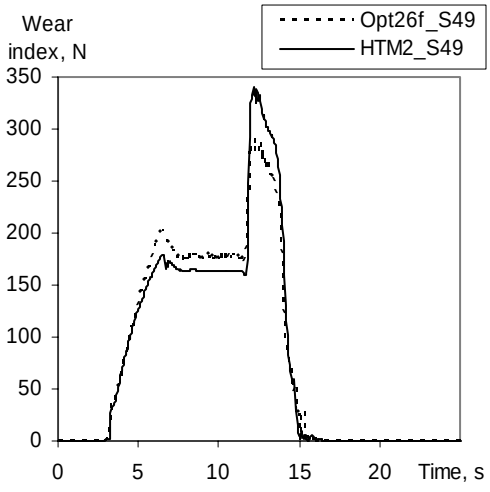

Fig. 11. Wear index of the left front wheel vs. time. Opt26f and HTM2 wheels are on S49 rail

6. Conclusions

The paper presents a procedure for design of

wheel profiles based on the rolling radii difference function. The wheel profiles with in advance defined geometrical contact properties have been obtained using a numerical optimization technique.

Using this procedure an optimized wheel profile for a tram has been obtained. Vehicle behaviour with the existing and obtained wheel profiles has been simulated on straight and curve tracks. It has been shown that the obtained wheel profile can reduce wheel/rail wear without deterioration of dynamic performance. The dynamic performance of the tram has been analysed using ADAMS/Rail computational package.

In application of wheel design for conventional trains the target RRD curve should be different since the running speed is higher (critical speed is more important) and curves of the railway lines are less sharp.

However, modification of wheel profiles is not the only method to solve the problems with wear and instability of vehicles. Engineers should keep in mind all factors influencing the vehicle dynamic, wear, maintenance costs etc. To solve such complex problems, optimization methods should be extensively used.

7. Acknowledgments

The authors would like to thank HTM (The Hague tram company) for providing measured data of wheel and rail profiles and tram model data. The profiles of wheel and rails were measured using MINIPROF measuring devices, manufactured by Greenwood Engineering (Denmark), whose assistance is greatly appreciated.

BIBLIOGRAPHY

[1] Dukkipati, R.V. 2000. Vehicle Dynamics, Boca Raton: CRC Press, ISBN 0-8493-0976-X.

[2] Esveld, C. 2001. Modern Railway Track, (Second Edition), Zaltbommel: MRT-Productions, ISBN 90-8004-324-3-3.

[3] Wickens, A.H. 1965. The Dynamic Stability of Railway Vehicle Wheelsets and Bogies Having Profiled Wheels, International Journal of Solids Structures 1: 319-341.

[4] Cooperrider, N.K. & Law, E.H. et al., 1976. Analytical and Experimental Determination of Nonlinear Wheel/Rail Constraints, Proceedings ASME Symposium on Railroad Equipment Dynamics.

[5] Pater, A.D. de 1988. The Geometrical Contact Between Track and Wheelset, Vehicle System Dynamics 17: 127-140.

[6] Markine, V.L. 1999. Optimization of the Dynamic Behaviour of Mechanical Systems, PhD Thesis, TU Delft: Shaker Publishing BV, ISBN 90-423-0069-8.

[7] Toropov, V.V. 1989. Simulation Approach to Structural Optimization, Structural Optimization 1: 37-46.

[8] Barthelemy, J.-F.M. & Haftka, R.T. 1993. Approximation Concept for Optimum Structural Design – a Review, Structural Optimization 5: 129-144.

[9] Toropov, V.V. & Markine V.L., 1996. The Use of Simplified Numerical Models as Mid-Range Approximations, Proceedings of the 6-th AIAA/USAF/NASA/ISSMO Symposium on Multidisciplinary Analysis and Optimization, Part 2, Bellevue WA, September 4-6, 1996: 952-958, ISBN 1-56347-218-X.

[10] Toropov, V.V., Keulen, F. van, Markine, V.L. & Alvarez, L.F. 1999. Multipoint Approximations Based on Response Surface Fitting: a Summary of Recent Developments. In V.V. Toropov (Ed.) Proceedings of the 1st ASMO UK/ISSMO Conference on Engineering Design Optimization, Ilkley, West Yorkshire, UK, July 8-9, 1999: 371-381, ISBN 0-86176-650-4.

[11] Kalker, J.J. 1990. Three-Dimensional Elastic Bodies in Rolling Contact, Dordrecht: Kluwer Academic Publishers, ISBN 0-7923-0712-7.

[12] Shevtsov, I.Y., Markine, V.L. & Esveld, C. 2002. One procedure for optimal design of wheel profile, Proceedings of the IQPC conference on Achieving Best Practice in Wheel/Rail Interface Management, Amsterdam, The Netherlands, January 31 - February 1, 2002.

[13] Shevtsov, I.Y., Markine, V.L & Esveld, C. 2003. Optimal design of wheel profile for railway vehicles, Proceedings 6th International Conference on Contact Mechanics and Wear of Rail/Wheel Systems, Gothenburg, Sweden, June 10-13, 2003: 231-236, ISBN 91-631-3928-6.